Frequency-comb-referenced singly-resonant OPO for sub-Doppler spectroscopy

I. Ricciardi,[1] E. De Tommasi,[1] P. Maddaloni,[1] S. Mosca,[1] A. Rocco,[1] J.-J. Zondy,[2] M. De Rosa,[1,*] and P. De Natale[1]

[1]*INO–CNR, Istituto Nazionale di Ottica, Sezione di Napoli, and LENS, European Laboratory for Nonlinear Spectroscopy, Via Campi Flegrei 34, I-80078 Pozzuoli (NA), Italy*
[2]*Laboratoire Commun de Métrologie LNE-CNAM, 61 rue du Landy, 93210 La Plaine Saint-Denis, France*
[*]*maurizio.derosa@ino.it*

Abstract: We present a widely-tunable, singly-resonant optical parametric oscillator, emitting more than 1 W between 2.7 and 4.2 μm, which is phase locked to a self-referenced frequency comb. Both pump and signal frequencies are directly phase-locked to the frequency comb of a NIR-emitting fs mode-locked fibre laser, linked, in turn, to the caesium primary standard. We estimate for the idler frequency a fractional Allan deviation of $\sim 3\times10^{-12}\tau^{-1/2}$ between 1 and 200 s. To test the spectroscopic performance of the OPO, we carried out saturation spectroscopy of several transitions belonging to the ν_1 rovibrational band of CH_3I, resolving their electronic quadrupole hyperfine structure, estimating a linewidth better than 200 kHz FWHM for the idler, and determining the absolute frequency of the hyperfine components with a 50-kHz-uncertainty.

OCIS codes: (190.4970) Parametric oscillators and amplifiers; (300.6320) Spectroscopy, high-resolution; (020.2930) Hyperfine structure.

References and links

1. F. Kühnemann, K. Schneider, A. Hecker, A. A. E. Martis, W. Urban, S. Schiller, and J. Mlynek, "Photoacoustic trace-gas detection using a cw single-frequency parametric oscillator," Appl. Phys. B **66**, 741–745 (1998)
2. A. Hecker, M. Havenith, C. Braxmaier, U. Strößner, and A. Peters, "High resolution Doppler-free spectroscopy of molecular iodine using a continuous wave optical parametric oscillator," Opt. Commun. **218**, 131–134 (2003).
3. M. M. J. W. van Herpen, S. E. Bisson, and F. J. M. Harren, "Continuous-wave operation of a single-frequency optical parametric oscillator at 45 μm based on periodically poled $LiNbO_3$," Opt. Lett. **28**, 2497–2499 (2003).
4. G. von Basum, D. Halmer, P. Hering, M. Mürtz, S. Schiller, F. Müller, A. Popp, and F. Kühnemann, "Parts per trillion sensitivity for ethane in air with an optical parametric oscillator cavity leak-out spectrometer," Opt. Lett. **29**, 797–799 (2004).
5. A. K. Y. Ngai, S. T. Persijn, G. Von Basum, and F. J. M. Harren, "Automatically tunable continuous-wave optical parametric oscillator for high-resolution spectroscopy and sensitive trace-gas detection," Appl. Phys. B **85**, 173–180 (2006).
6. H. Verbraak, A. K. Y. Ngai, S. T. Persijn, F. J. M. Harren, and H. Linnartz, "Mid-infrared continuous wave cavity ring down spectroscopy of molecular ions using an optical parametric oscillator," Chem. Phys. Lett. **442**, 145–149 (2007).
7. D. D. Arslanov, S. Cristescu, and F. J. M. Harren, "Optical parametric oscillator based off-axis integrated cavity output spectroscopy for rapid chemical sensing," Opt. Lett. **35**, 3300–3302 (2010).
8. S. Persijn, F. Harren, and A. Veen, "Quantitative gas measurements using a versatile OPO-based cavity ringdown spectrometer and the comparison with spectroscopic databases," Appl. Phys. B **100**, 383–390 (2010).

#162465 - $15.00 USD Received 8 Feb 2012; revised 22 Mar 2012; accepted 26 Mar 2012; published 5 Apr 2012

9. D. D. Arslanov, M. Spunei, A. K. Y. Ngai, S. M. Cristescu, I. D. Lindsay, S. T. Persijn, K.-J. Boller, and F. J. M. Harren, "Rapid and sensitive trace gas detection with continuous wave optical parametric oscillator-based wavelength modulation spectroscopy" Appl. Phys. B **103**, 223–228 (2011).
10. E. V. Kovalchuk, D. Dekorsy, A. I. Lvovsky, C. Braxmaier, J. Mlynek, A. Peters, and S. Schiller, "High-resolution Doppler-free molecular spectroscopy with a continuous-wave optical parametric oscillator," Opt. Lett. **26**, 1430–1432 (2001).
11. H. Inaba, T. Ikegami, F.-L. Hong, Y. Bitou, A. Onae, T. R. Schibli, K. Minoshima, and H. Matsumoto, "Doppler-free spectroscopy using a continuous-wave optical frequency synthesizer," Appl. Opt. **45**, 491–4915 (2006).
12. S. Zaske, D.-H. Lee, and C. Becher, "Green-pumped cw singly resonant optical parametric oscillator based on MgO:PPLN with frequency stabilization to an atomic resonance," Appl. Phys. B **98**, 729–735 (2010).
13. M. Vainio, M. Siltanen, J. Peltola, and L. Halonen, "Grating-cavity continuous-wave optical parametric oscillators for high-resolution mid-infrared spectroscopy," Appl. Opt. **50**, A1–A10 (2011).
14. M. Vainio, M. Merimaa, and L. Halonen, "Frequency-comb-referenced molecular spectroscopy in the mid-infrared region," Opt. Lett. **36**, 4122–4124 (2011).
15. P. Maddaloni, G.Gagliardi, P. Malara, and P. De Natale, "A 3.5-mW continuous-wave difference-frequency source around 3 μm for sub-Doppler molecular spectroscopy," Appl. Phys. B **80**, 141–145 (2005).
16. I. Galli, S. Bartalini, S. Borri, P. Cancio Pastor, G. Giusfredi, D. Mazzotti, and P. De Natale, "Ti:sapphire laser intracavity difference-frequency generation of 30 mW cw radiation around 4.5 μm," Opt. Lett. **35**, 3616–3618 (2010).
17. S. Okubo, H. Nakayama, and H. Sasada, "Hyperfine-resolved 3.4-μm spectroscopy of CH_3I with a widely tunable difference frequency generation source and a cavity-enhanced cell: a case study of a local Coriolis interaction between the $\nu_1 = 1$ and $(\nu_2, \nu_6^l) = (1, 2^2)$ states," Phys. Rev. A **83**, 012505 (2011).
18. I. Ricciardi, E. De Tommasi, P. Maddaloni, S. Mosca, A. Rocco, J.-J. Zondy, M. De Rosa, P. De Natale, "A singly-resonant optical parametric oscillator for mid-infrared high-resolution spectroscopy," submitted to Molecular Physics (2012).
19. R. F. Curl, F. Capasso, C. Gmachl, A. A. Kosterev, B. McManus, R. Lewicki, M. Pusharsky, G. Wysocki, and F. K. Tittel, "Quantum cascade lasers in chemical physics," Chem. Phys. Lett. **487**, 1–18 (2010).
20. S. Borri, S. Bartalini, P. Cancio, I. Galli, G. Giusfredi, D. Mazzotti, and P. De Natale, "Quantum cascade lasers for high-resolution spectroscopy," Opt. Eng. **49**, 111122 (2010).
21. E. V. Kovalchuk, T. Schuldt, and A. Peters, "Combination of a continuous-wave optical parametric oscillator and a femtosecond frequency comb for optical frequency metrology," Opt. Lett. **30**, 3141–3143 (2005).
22. J. L. Hall and J. A. Magyar, "High-resolution saturated absorption studies of methane and some methyl-halides," in *High Resolution Laser Spectroscopy*, K. Shimoda, ed. (Springer-Verlag, 1976), pp. 173–199.
23. P. Maddaloni, P. Cancio, and P. De Natale, "Optical comb generators for laser frequency measurement," Meas. Sci. Technol. **20**, 052001 (2009).
24. C. H. Townes and A. L. Schawlow, *Microwave Spectroscopy* (Dover, 1975).
25. R. Paso, V. M. Horneman, and R. Anttila, "Analysis of the ν_1 band of CH_3I," J. Mol. Spectrosc. **101**, 193–198 (1983).
26. G. Buffa, A. Di Lieto, P. Minguzzi, O. Tarrini, and M. Tonelli, "Nuclear-quadrupole effects in the pressure broadening of molecular lines," Phys. Rev. A **37**, 3790–3794 (1988).
27. K. Schneider and S. Schiller, "Narrow-linewidth, pump-enhanced singly-resonant parametric oscillator pumped at 532 nm," Appl. Phys. B **65**, 775–777 (1997).
28. U. Strössner, J.-P. Meyn, R. Wallenstein, P. Urenski, A. Arie, G. Rosenman, J. Mlynek, S. Schiller, and A. Peters, "Single-frequency continuous-wave optical parametric oscillator system with an ultrawide tuning range of 550 to 2830 nm," J. Opt. Soc. Am. B **19**, 1419–1424 (2002).
29. P. Maddaloni, P. Malara, E. De Tommasi, M. De Rosa, I. Ricciardi, G. Gagliardi, F. Tamassia, G. Di Lonardo, and P. De Natale, "Absolute measurement of the S(0) and S(1) lines in the electric quadrupole fundamental band of D_2 around 3 μm," J. Chem. Phys. **133**, 154317 (2010).

1. Introduction

Continuous wave optical parametric oscillators (OPOs) are coherent sources of radiation having unique features, for a wide range of different applications. Indeed, singly resonant OPOs combine high power, single mode emission, tunability, and wide spectral coverage from visible to mid infrared (MIR). These characteristics make cw OPOs attractive for atomic and molecular spectroscopy. They are easier to operate with respect to doubly resonant or pump-resonant OPOs, although they have a higher threshold power, typically in the Watt range.

In the last years, improvements in the efficiency of nonlinear materials and availability of powerful and narrow-linewidth near-infrared (NIR) lasers have led to different OPO configu-

#162465 - $15.00 USD Received 8 Feb 2012; revised 22 Mar 2012; accepted 26 Mar 2012; published 5 Apr 2012

rations for high-resolution and accurate spectroscopic applications [1–9], demonstrating sub-Doppler resolution in the near- and mid-infrared [10–14]. In this region, difference frequency generation (DFG) sources also showed wide tunability and narrow spectral emission, typically emitting few milliWatts in single passage or few tens of mW in intracavity configuration [15–17]. Quantum cascade lasers are relentlessly improving their performances, providing tunability over $\sim$100 cm^{-1}, narrow linewidth, with hundreds-mW-level cw emission at room temperature, covering the whole MIR range with few gaps, proving to be useful for high resolution spectroscopy [19, 20]. With respect to such sources, OPOs have even wider tunability and more power, with comparable spectral resolution. Moreover, OPOs emitting in the MIR have been combined with visible and NIR optical frequency comb (OFC) synthesizers, providing high-precision and absolute frequency determination outside of the specific OFC covered range [11, 14, 21]. In particular, focusing our discussion on the MIR range, Kovalchuk et al. demonstrated simultaneous phase-locking of a pump- and signal-resonant OPO to a Ti:sapphire OFC [21]. More recently, Vainio et al. referenced a singly resonant OPO to a Ti:sapphire frequency comb. In both cases signal frequency was outside of the frequency comb range. So, they had to use residual non-phase-matched components which are usually generated in the OPO crystal, to stabilize the pump-signal frequency difference. In one case [14] the authors do not use the comb teeth which should be available at 1064 nm, but they expressly use a second nonlinear crystal, generating the second harmonics of the pump which, in turn, beats with the green part of the comb. Moreover, the beat notes between harmonics and the corresponding nearest comb teeth were frequency counted and the counter readings used as error signals for frequency control of pump laser and OPO cavity.

Here we present a singly resonant cw OPO, emitting more than 1 W in the MIR range, between 2.7 and 4.2 μm, which has been directly frequency locked to a near-infrared self-referenced OFC with an octave-span from 1 to 2 μm, without the help of intermediate frequencies, since both pump (1.064 μm) and signal (1.4-1.7 μm) frequencies are in the range of the OFC. To test the spectral features of such source we performed sub-Doppler spectroscopy of ν_1 band rovibrational transitions of methyl iodide (CH_3I) around 3.3 μm, resolving their electronic quadrupole hyperfine structure and estimating an upper limit of 200 kHz for the idler linewidth FWHM (hereafter all the reported linewidths are FWHM). Sub-Doppler spectroscopy of this band was previously performed, in a narrower frequency range, by intracavity spectroscopy with a CH_4-stabilized HeNe laser [22] and, more recently, Okubo et al. observed the hyperfine structure of several transitions around 3.4 μm, using a DFG source and a cavity-enhanced sub-Doppler scheme [17].

2. Experimental setup

Our OPO, Fig. 1, is pumped by a narrow-linewidth (40 kHz over 1 ms) cw Yb-doped fibre laser, emitting at 1064 nm, amplified by a Yb-doped fibre amplifier up to 10 W. The OPO is typically pumped by the whole emitted power. Laser frequency can be finely tuned over a few GHz by acting on a piezoelectric actuator which changes the fibre cavity length. Coarse tuning can be achieved by changing the temperature of the laser cavity. Few milliWatts from the laser beam are separately sent to a 50-MHz-resolution wavemeter and to a fibre-coupled electro-optic phase modulator (EOM) which adds two sidebands at frequency $\pm f_{\mathrm{EOM}}$ with respect to the laser carrier frequency ν_p. In this way, the laser can be locked to the frequency comb through a sideband, while the carrier frequency, which pumps the OPO, can be scanned by changing the driving frequency f_{EOM}, thus allowing sweeps across molecular lines (see Sec.s 2.2 and 3). About 70 mW of laser power (pump beam) is sent to the amplifier through an optical fibre and acts as pump beam for the OPO. A two-stage optical isolation system is used before and after the amplifier, to avoid optical feedback.

#162465 - $15.00 USD Received 8 Feb 2012; revised 22 Mar 2012; accepted 26 Mar 2012; published 5 Apr 2012

2.1. The optical parametric oscillator

The OPO cavity is made by four mirrors in a bow-tie configuration, with two curved (100 mm of radius of curvature) and two plane mirrors, Fig. 1(b). The effective length of the cavity is 695 mm, corresponding to a free spectral range of 430 MHz. All the mirrors have a high reflective coating for the signal wavelength ($R > 99.9\%$) between 1410 and 1800 nm. Curved mirrors have high-transmission coating for pump ($R < 2\%$) and idler wavelength ($R < 5\%$).

The crystal is a sample of 5%-MgO-doped congruent lithium niobate, 50-mm-long and 1-mm-thick, with seven different poling periods ranging from 28.5 to 31.5 μm. The crystal end facets have anti-reflection coating for the pump ($R < 3\%$ at 1064 nm) and the signal ($R < 1\%$ in the range 1450-1850 nm) and high transmission coating for the idler ($R < 10\%$ in the range 2500-4000 nm). The crystal is enclosed in a temperature-controlled oven, with 0.1°C stability, mounted on a mechanical positioner, and placed at the centre between the two curved mirrors, in correspondence of the smallest cavity waist. The pump radiation is coupled into the cavity through one of the curved mirrors and focused at the centre of the nonlinear crystal with a beam waist w_p of 48 μm. The beam waist w_s for the signal wave varies from 53 μm at 1.4 μm, to 60 μm at 1.8 μm, so that pump and signal have approximately the same confocal beam parameter.

An adjustable 400-μm-thick uncoated YAG etalon is placed between the two flat mirrors for reducing mode-hops of the signal oscillation. A Germanium (Ge) filter is used to separate the MIR idler beam from visible and NIR components. Signal light leaking through one of the cavity mirrors is coupled into an optical fibre and made available for signal locking and frequency measurement.

The OPO cavity is mounted on a dedicated breadboard placed on four rubber chunks, and covered by a plexiglass enclosure for protection against dust, air currents, and acoustic and mechanical disturbances.

The OPO has been characterized [18] in the range between 2.7 and 4.2 μm, where it emits typically about 1 W of MIR power with 10 W of pump power. At longer wavelengths the power tends to decrease, both due to the intrinsic dependence of the nonlinear efficiency on the wavelength and to the decrease of cavity mirror reflectivity for the signal. The threshold at 2.9 μm has been determined as 3 W. The OPO typically operates without mode-hops for about 30 minutes. At the moment no effort has been spent to improve these figures. Idler tuning without mode hops over three GHz is achieved by acting on the laser piezo, mantaining the OPO cavity stable. Coarser tuning of the OPO can be realized by changing either the laser or the nonlinear crystal temperature.

2.2. Phase-lock to the optical frequency comb

To obtain stable idler emission with absolutely known frequency, both pump and signal frequencies are locked to a self-referenced OFC synthesizer (Menlo systems, FC1500). Our OFC synthesizer is based on an amplified mode-locked Er:doped fibre laser, followed by a nonlinear photonic fibre which generates an octave-spanning (between 1–2 μm) frequency comb of 250-MHz-spaced modes (corresponding to the laser repetition rate f_r). An $f-2f$ beat unit allows continuous monitoring of the carrier-envelope offset frequency f_ceo. Thus, the frequency of each mode N can be written as $\nu_N = N f_\mathrm{r} + f_\mathrm{ceo}$. Repetition rate and offset frequency are stabilized against a 10 MHz BVA quartz, locked to a Rb-clock, referenced to the Cs primary standard via global positioning system.

Radiation from the comb is coupled into two optical fibres and combined with few mW of pump and signal light, respectively (Fig. 1(a)). The beat note f_b1 (f_b2) between pump (signal) and the nearest comb tooth is detected by a PIN-InGaAs fast photodiode, mixed with a local oscillator (LO) at frequency $f_\mathrm{LO1} = 12$ MHz ($f_\mathrm{LO2} = 12$ MHz) and sent to an electronic servo

#162465 - $15.00 USD Received 8 Feb 2012; revised 22 Mar 2012; accepted 26 Mar 2012; published 5 Apr 2012

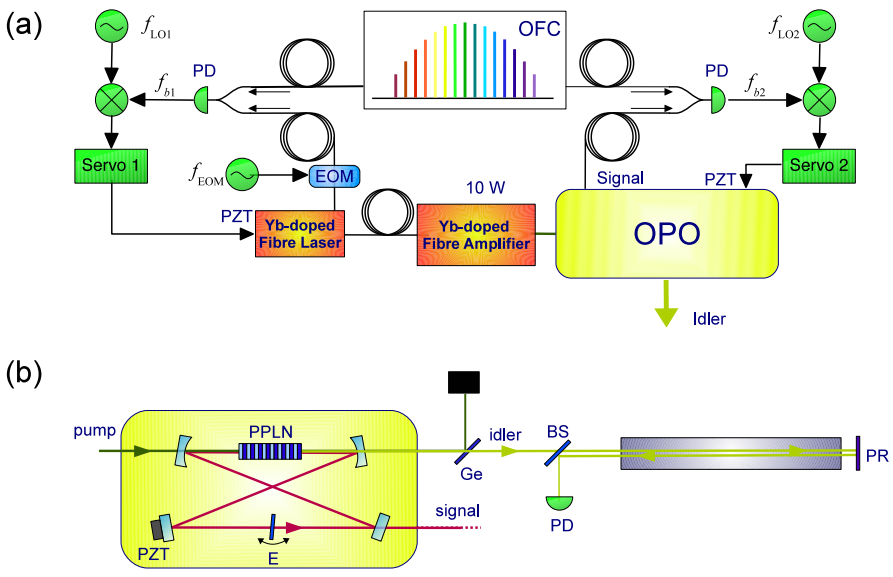

Fig. 1. (a) Simplified scheme of the OPO phase-locking to the optical frequency comb (OFC). (b) Scheme of the OPO four-mirrors ring cavity and saturation spectroscopy setup. PPLN: periodically-poled lithium niobate crystal; PZT: piezoelectric actuator; E: YAG etalon; Ge: germanium filter; BS: 98%-transmission beam splitter; PD: photodiode; PR: partial reflecting mirror.

which drives the laser (OPO) piezo actuator. Beat notes are band-pass filtered (9-15 MHz), to minimize noise contribution from other comb lines, and amplified, getting a S/N ratio better than 30 dB, measured with 30 kHz of resolution bandwidth. Both servos have a unity gain bandwidth of ~ 100 Hz, and residual phase power spectral density less than 0.1 rad^2/Hz in the locking range. Frequency counters are used to count f_{b1}, f_{b2}, and f_r, while the wavemeter measures the pump and signal wavelength after locking. Frequency counters and frequency synthesizers generating f_{LO1}, f_{LO2} and f_{EOM} are all referenced to the BVA-defined time base. Counters' gate time is set to 1 s, however, a dead time between two successive readings is added by the acquisition routine, leading to a sample time of more than two seconds, depending on the number of the counted signals.

For the pump, we lock one of the laser sidebands, e.g., $\nu_p - f_{EOM}$, while the OPO is pumped at ν_p. In this way, by changing the EOM frequency f_{EOM}, the idler frequency can be scanned over 70 MHz, while mantaining the laser locked to the OFC. Thus, pump and signal frequencies can be written as $\nu_p = f_{ceo} + N_p f_r + f_{b1} + f_{EOM}$ and $\nu_s = f_{ceo} + N_s f_r + f_{b2}$, respectively [23], and the idler frequency is given by

$$\nu_i = \nu_p - \nu_s = (N_p - N_s) f_r + f_{b1} - f_{b2} + f_{EOM}\,. \tag{1}$$

We remark that the offset frequency cancels in Eq. (1), and in principle it is not necessary to stabilize it for absolute determination of the idler frequency.

N_p and N_s are determined every time the OPO was locked, by measuring pump and signal wavelengths by means of the calibrated wavemeter. As a countercheck, we acquired spectra at different values for the repetition frequency f_r.

From counter readings we calculated the Allan deviation for f_{b1}, f_{b2}, and $(N_p - N_s)\, f_r$ which contribute to the final stability of the idler frequency. Allan deviations Fig. (2), are well fitted

#162465 - $15.00 USD Received 8 Feb 2012; revised 22 Mar 2012; accepted 26 Mar 2012; published 5 Apr 2012

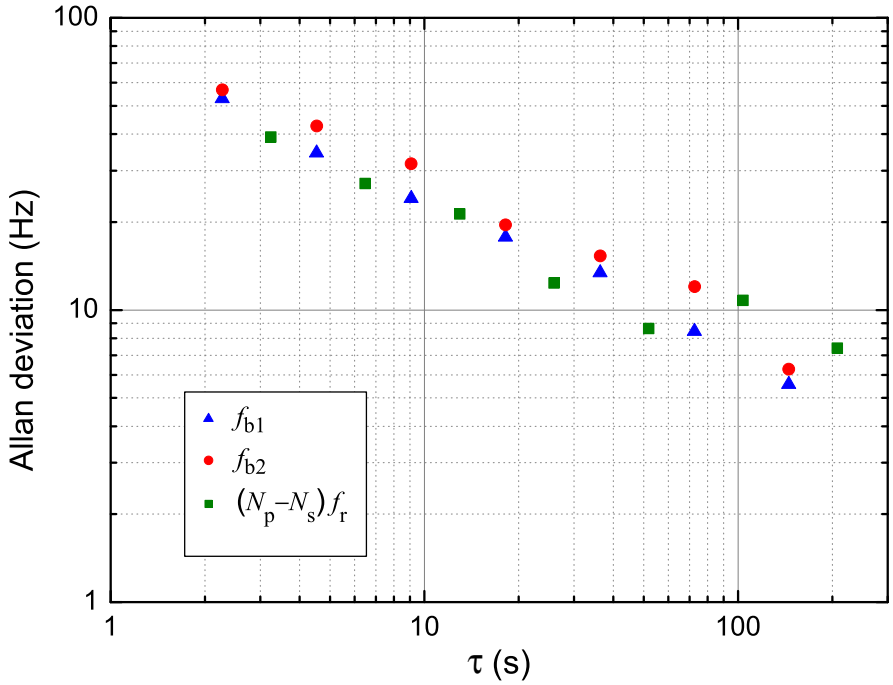

Fig. 2. Allan deviation of the three relevant contributions to the idler frequency (see Eq. 1). The gate time of the frequency counters is 1 s.

by a $\sigma_o \tau^{1/2}$ law with 1-s-stability σ_o of 80, 90, and 70 Hz for f_{b1}, f_{b2}, and $(N_p - N_s)\, f_r$, respectively. Assuming significant correlation amongst the three frequencies, we can conservatively estimate a final relative frequency stability for the idler $\lesssim 3 \times 10^{-12}\, \tau^{-1/2}$, for τ between 1 and 200 s.

3. Sub-Doppler spectroscopy

For sub-Doppler spectroscopy, the sample contained in a 50-cm-long cell, Fig. 1(b), is saturated by the linearly-polarized, collimated idler beam (0.7-mm waist at the end of the cell). A partial-reflecting mirror, PR, reflects back a small fraction of radiation, which probes the saturated absorption and is deviated towards a thermoelectric-cooled HgCdTe photodetector by a 98% -transmission beam splitter, BS. The cell is connected to a vacuum pump for gas evacuation and to a CH_3I reservoir for refilling. A 1-Torr-full-scale capacitive pressure gauge monitors the pressure inside the cell. To increase the sensitivity to small saturation dips, we adopted $1f$ phase-sensitive detection. For this purpose, a 15 kHz (larger than phase-lock bandwidths) voltage modulation is added to the laser PZT for frequency modulation and the detector signal is sent to a lock-in amplifier for $1f$ demodulation.

The pump laser is initially scanned across the molecular line, by applying a voltage ramp to the laser PZT. Then, the signal is locked to the OFC and the laser frequency is carefully set near the center of the line and finally the laser sideband is locked, too. After locking pump and signal frequencies, calibrated frequency scans across spectral lines are made by changing the EOM-driving RF by discrete steps, pausing at least 3 times the integration time of the lock-in amplifier, and synchronously acquiring the demodulated absorption signal from the

#162465 - $15.00 USD Received 8 Feb 2012; revised 22 Mar 2012; accepted 26 Mar 2012; published 5 Apr 2012

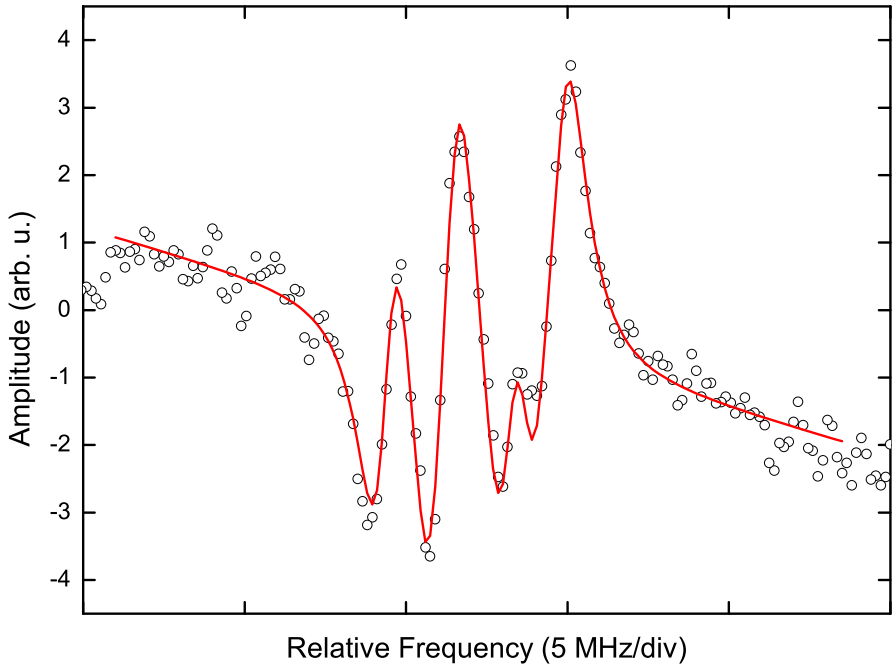

Fig. 3. Sub-Doppler-resolved hyperfine structure of the ν_1 P(18,3) ro-vibrational transition of CH_3I, at 30 mTorr pressure and with 630 mW of saturating power. Experimental data (open squares) have been fitted by a linear background and six Lorentian derivatives, with equal widths and amplitudes (solid line).

lock-in together with counters' records. Frequency scans are made both forward and backward across the lines, and data from both scans are averaged to compensate for artificial distortion introduced by lock-in integration.

Each rovibrational level, identified by the two rotational quantum numbers J and K, is splitted by electric quadrupole interaction of the iodine nucleus (nuclear spin, $I = 5/2$) into hyperfine sublevels, identified by total angular moment $\mathbf{F} = \mathbf{J} + \mathbf{I}$, with $F = |J - I|, ..., J + I$ [24]. These hyperfine sublevels give rise to transitions satisfying the selection rule $\Delta F = \Delta J$.

As an example, Fig. 3 shows a $1f$ signal of the resolved hyperfine structure of the saturated ν_1 P(18,3) rovibrational transition at the pressure of 30 mTorr and with 630 mW of saturating power. Line assignment is based on molecular constants determined by FTIR analysis [25]. No accurate data are present in the literature about the line intensity for this region. We roughly estimate for line P(18,3) an intensity of $\sim 4.3 \times 10^{-21}$ cm/mol. The profile has been fitted by a linear background and six Lorentian profile derivatives with equal widths and amplitudes. From the fit we retrieve a value of 1640 ± 60 kHz for the Lorentian full-width and the absolute frequencies of the hyperfine components. The centroid of the multiplet is $88\,791\,204.19 \pm 0.05$ MHz. The reported uncertainty is the standard deviation of the fit results from different data sets and it could represents only a part of the overall uncertainty on the frequency estimate. We did not take into account systematic effects (AC Stark shift, pressure shift, etc.), which could contribute to the final uncertainty budget.

In Table 1 we resume the measured position of the six components with respect to the centroid and the corresponding theoretical values calculated on the basis of the recently re-

#162465 - $15.00 USD Received 8 Feb 2012; revised 22 Mar 2012; accepted 26 Mar 2012; published 5 Apr 2012

Table 1. Measured absolute frequencies of the six hyperfine components of ν_1 P(18,3) rovibrational transition, given as relative position with respect to the centroid frequency of the multiplet, 88 791 204.19 ± 0.05 MHz. Errors on the last significative digits (in parentheses) are the standard deviations of the fit results from different data sets. Theoretical values are reported for comparison.

$F'' \rightarrow F'$	Measured (MHz)	Calculated (MHz)
$\frac{31}{2} \rightarrow \frac{29}{2}$	−1.03 (6)	−1.13
$\frac{33}{2} \rightarrow \frac{31}{2}$	1.95 (5)	1.95
$\frac{35}{2} \rightarrow \frac{33}{2}$	2.39 (3)	2.33
$\frac{37}{2} \rightarrow \frac{35}{2}$	0.88 (6)	0.93
$\frac{39}{2} \rightarrow \frac{37}{2}$	−1.26 (6)	−1.20
$\frac{41}{2} \rightarrow \frac{39}{2}$	−2.92 (3)	−2.88

fined quadrupole coupling constants [17]. The centroid value is compatible with the value of 88 791 230 ± 120 MHz calculated on the basis of Ref. [25]. The relative positions of the six components are in good agreement with the calculated ones.

We estimate a collisional linewidth of ∼ 640 kHz at 30 mTorr [26] and a transit-time contribution of 100 kHz for a Gaussian beam waist of 0.7 mm. Also, we acquired different profiles of the same hyperfine multiplet by separately changing saturating power and modulation depth, to estimate their contributions to the final linewidth. We got 260 kHz for the modulation broadening and 440 kHz due to power broadening for 630 mW of saturating power. In the end, we can estimate an upper limit of 200 kHz for the idler linewidth. The main contribution to the final linewidth is due to the signal frequency fluctuations, induced by residual mechanical noise (up to ∼ 2 kHz) of the OPO cavity outside of the servo bandwidth. A comparison with other OPOs is not straightforward, as linewidths have been inferred by different methods and on different time scales, depending on the particular application, resulting in values in the 10–100 KHz range on relatively short time scales (10–500 μs) [6, 10, 27, 28]. In an application similar to ours [17], DFG source contribution to the spectral resolution of the hyperfine transitions is less than 200 KHz.

4. Conclusions

We have reported on a singly resonant OPO, pumped at 1064 nm and emitting more than 1 W between 2.7 and 4.2 μm, which has been referenced to a frequency comb in the NIR, linked to the caesium frequency standard. Relative frequency stability of $\sim 3 \times 10^{-12} \tau^{1/2}$ for τ between 1 and 200 s has been estimated for the idler. As a spectroscopic test, we observed sub-Doppler profiles of several CH_3I rovibrational transitions, resolving their hyperfine structure and determining the absolute frequencies of the multiplet components with an uncertainty of 50 kHz. We also estimate an upper limit of 200 kHz for the source linewidth. However, a detailed investigation of the different contributions to the final linewidth is needed, even though preliminary measurements indicate that an improvement of the locking bandwidths can appreciably improve the OPO spectral characteristics. The combination of high power, narrow linewidth, and precise and absolute frequency control over a wide range of tunability makes this source a valuable and versatile tool for high-resolution spectroscopy in a spectral region of growing interest for many applications and accurate tests of fundamental theoretical models [29].

#162465 - $15.00 USD Received 8 Feb 2012; revised 22 Mar 2012; accepted 26 Mar 2012; published 5 Apr 2012

Acknowledgments

The authors thank Gianluca Notariale for technical help. This work was partially supported by Regione Toscana through the project SIMPAS, in the framework of PORCReO FESR 2007-2013.

#162465 - $15.00 USD Received 8 Feb 2012; revised 22 Mar 2012; accepted 26 Mar 2012; published 5 Apr 2012